Electrical conductivity of Cr_2O_3-doped Y_2O_3-stabilized ZrO_2

MANIKPRAGE JAYARATNA, MASAHIRO YOSHIMURA, SHIGEYUKI SŌMIYA
Research Laboratory of Engineering Materials and Department of Materials Science, Tokyo Institute of Technology, 4259 Nagatsuta, Midori, Yokohama 227, Japan

The electrical conductivity of Cr_2O_3-doped Y_2O_3-stabilized ZrO_2 (YSZ) has been studied as functions of composition, temperature and oxygen pressure. The specimens have been prepared by hot pressing of co-precipitated oxides to yield >99.7% density. The Cr_2O_3 added above the solubility limit ($\approx$0.7 mol%) precipitated as a secondary phase at the grain boundaries. The conductivity of Cr_2O_3-doped YSZ was almost independent of the oxygen pressure in the range 10^{18} to 10^5 Pa, indicating a dominant ionic condition. The electronic conductivity of dopant Cr_2O_3 would be hindered by the higher ionic conductivity in the p_{O_2} ranges studied. The conductivity and the activation energy for conduction decreased slightly with the addition of Cr_2O_3. These phenomena seemed to be caused by vacancy trapping or polarization at the grain boundaries with the Cr_2O_3 precipitates. The samples with 1 mol% Cr_2O_3 added to zirconia containing various Y_2O_3 contents showed similar conduction behaviour to those without Cr_2O_3 addition; that is, the conductivity maxima are observed at around 8 mol% Y_2O_3 addition to zirconia, and the activation energies increased with the Y_2O_3 addition.

1. Introduction

It is generally accepted that stabilized ZrO_2 is a defect solid solution with oxygen vacancies [1, 2] and electrical conduction occurs due to the mobility of oxygen ions at higher temperatures. This ionic conductivity has led to the applications of stabilized ZrO_2 in galvanic cells, oxygen sensors, fuel cells, etc. Among ZrO_2 electrolytes Y_2O_3-stabilized ZrO_2 is considered to be better than CaO- or MgO-stabilized ZrO_2, in view of its higher conductivity and the stability over a wide temperature range. A maximum conductivity for Y_2O_3-stabilized ZrO_2 has been reported by Dixon *et al.* [3] and Strickler and Carlson [4] at the cubic–tetragonal phase boundary (8 to 9 mol% Y_2O_3). Furthermore the conductivity of Y_2O_3-stabilized ZrO_2 remains constant, exhibiting pure ionic conductivity over a wide range of oxygen partial pressures [5].

Studies on the conductivity of stabilized ZrO_2 with various additives have been of interest to investigators for the applications of stabilized ZrO_2 in sensors [6], mixed conductors [7, 8], etc. The mixed conductors obtained from Y_2O_3-stabilized ZrO_2 are excellent conductors for hydrogen production from steam and for rechargeable batteries. Anthony [9] and Browall and Doremus [8] reported that Cr_2O_3-doped Y_2O_3-stabilized ZrO_2 is one of the most promising mixed conductors in hydrogen production. They measured the a.c. conductivity and transference number for Cr_2O_3-doped Y_2O_3-stabilized ZrO_2 and reported a transference number of about 0.8 at 1000° C and 10^{-16} atm p_{O_2}. Karavaev *et al.* [10] also have reported electrical conductivity and transference numbers for materials in the ZrO_2–Y_2O_3–Cr_2O_3 system. However, these studies were limited to the transference number and conductivity measurement with temperature and they did not report the variation of conductivity with p_{O_2} and composition. Thus in the present study it was intended to measure the conductivity of Cr_2O_3-doped Y_2O_3-stabilized ZrO_2 with oxygen partial pressure, temperature and composition using pore-free samples prepared by hot pressing.

Previously we studied the phase relations in the system ZrO_2–Y_2O_3–Cr_2O_3 [11] and found that Cr_2O_3 is compatible with a ZrO_2 solid solution containing $\approx$17 mol% Y_2O_3. Again in a hot-pressing study [12] the solubility of Cr_2O_3 in 8 mol% Y_2O_3-stabilized ZrO_2 was found to be 0.7 mol% at 1450° C. The present paper describes the conductivity measurements of the materials in the system ZrO_2–Y_2O_3–Cr_2O_3.

2. Experimental procedure

2.1. Samples

The samples for conductivity measurements were prepared by the hot pressing of co-precipitated materials. The details of starting powder preparation and hot-pressing technique have been described in a previous paper [12]. All the samples for conductivity measurement were hot-pressed under the same condition at 1500° C, with 43.7 MPa pressure for 30 min in an argon atmosphere using graphite dies. Pellets of 10 mm diameter and 3 to 4 mm height were obtained by hot pressing. They were annealed first at 1200° C for 48 h in air to oxidize all contaminants from the die and metallic chromium produced by the reduction of Cr_2O_3 during hot pressing. Specimens of about 1.5 mm × 2.5 mm × 9 mm were then cut from those pellets to be used in conductivity measurements.

The density of hot-pressed samples was measured

0022–2461/87 $03.00 + .12

by Archimedes' method in mercury. Microstructural observations were done for the polished and etched (in boiling H_3PO_4) surfaces using scanning electron microscopy (SEM).

2.2. D.c. conductivity measurement

The d.c. four-probe method [13] was used for d.c. conductivity measurement. Platinum wires of 0.2 mm diameter were connected to the specimen as electrical probes through pressure contact. To eliminate the effect of surface currents, platinum paste was applied to both edge probes which were used to apply the current. Potential difference was measured between the central probes. The circuit used for conductivity measurement is shown in Fig. 1. The current through the specimen was measured by the ohmic drop across the standard resistor of 100 or 1000 Ω. All the voltages were measured with a high-impedance digital voltmeter. During the conductivity measurement, the specimen was suspended horizontally in a vertical tube furnace with an SiC double spiral heating element by means of four probes supported by an alumina holder. The temperature was measured by a Pt/Pt–13 Rh thermocouple calibrated to the melting points of palladium and gold and controlled within 1° C.

Oxygen partial pressure was controlled by H_2/CO_2 gas mixtures or by an O_2 pump. Partial oxygen pressure was measured by a zirconia oxygen sensor placed downstream of the furnace. The e.m.f. developed between both sides of the sensor as a result of p_{O_2} difference is

$$E = \frac{RT}{4F} \ln \frac{p_{O_2}}{p_{O_2 \text{ref.}}}$$

where R = gas constant, T = temperature, F = Faraday constant, and p_{O_2}, $p_{O_2 \text{ref.}}$ are the partial oxygen pressures in measured and reference gases, respectively. Air is used as the reference gas. The p_{O_2} at the specimen $T = T_{\text{specimen}}$ was obtained from the p_{O_2} at the sensor $T = T_{\text{sensor}}$ on calculations based upon the thermodynamical equilibrium constants [14] for each reaction between the gases in the gas mixture.

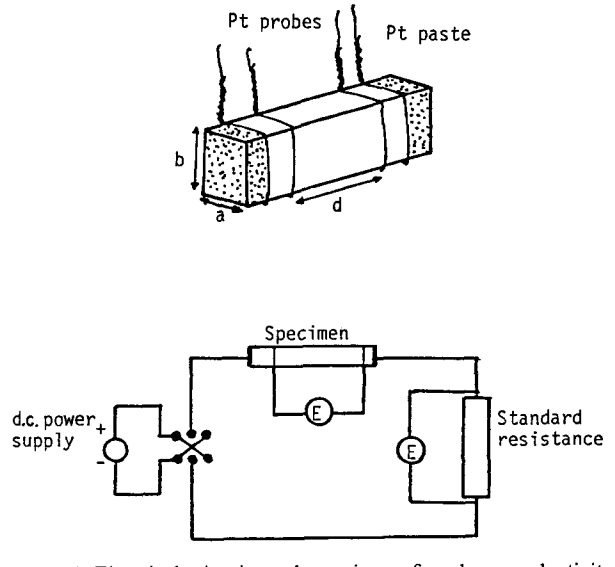

Figure 1 Electrical circuit and specimen for d.c. conductivity measurement. $\sigma = d/abR$.

2.3. Complex impedance measurement

The complex impedance of Cr_2O_3-doped YSZ was measured using a vector impedance meter. Annealed hot-pressed specimens of 10 mm diameter were used. Firstly platinum paste was applied to both sides and fired at 800° C. Then they were placed between two platinum electrodes of the equipment. The impedance and phase angle for various frequencies were read by direct meter readings at various temperatures.

3. Results and discussion

The densities and grain sizes of the samples used for conductivity measurements are given in Table I. All the samples had 99% of theoretical density and 1 to 9 μm grain sizes. The microstructures of the specimens showed secondary phase particles precipitated on the grain boundaries in samples containing more than 1 mol % Cr_2O_3. By energy-dispersive spectroscopy, these secondary-phase particles were found to be Cr_2O_3 precipitates. The microstructure and Cr$K\alpha$ X-ray image for a 3 mol % Cr_2O_3-doped sample is shown in Fig. 2. The secondary Cr_2O_3 phase can be seen in white among dark ZrO_2 solid-solution grains in Fig. 2. The microstructures and Cr$K\alpha$ X-ray images showed homogeneous Cr_2O_3 dispersion all over the specimen in addition to the precipitates on the grain boundaries.

3.1. Conductivity behaviour

The ohmic behaviour of the electrical conductivity was examined by changing the d.c. current from 0.6 to 15 mA cm^{-2}. Potential differences between each pair of probes were measured to examine the potential drop along the specimen. Almost all the results showed ohmic behaviour, but some cases exhibited a non-ohmic potential drop along the specimen. When $\log [p_{O_2}(\text{Pa})]$ was around zero such non-ohmic behaviour could generally be observed. As an example, Fig. 3 shows the observed potential differences in a CO_2 atmosphere. It shows a non-proportional relation between potential drop and the current at the cathode for both normal and reverse currents. The cathode process is represented by the reaction

$$2e' + \tfrac{1}{2}O_2 + V_o^{\cdot\cdot} = O_o$$

Thus it seems the cathode polarization occurs due to a very slow reaction at the cathode in low p_{O_2}. However, potential differences between the two middle probes showed linearity with current for both normal and reverse directions. This non-ohmic behaviour

TABLE I Density and grain sizes of the samples used for conductivity measurement, $(1-y)[(1-x)ZrO_2 + xY_2O_3] + yCr_2O_3$; samples hot-pressed at 1500° C under 43.7 MPa pressure for 30 min

Composition		Density (%)	Average grain size (μm)
x	y		
8	0	99.8	9
8	1	99.9	8
8	3	99.9	8
5	1	99.9	1
12	1	99.9	4
15	1	98.5	3
17	1	99.0	7

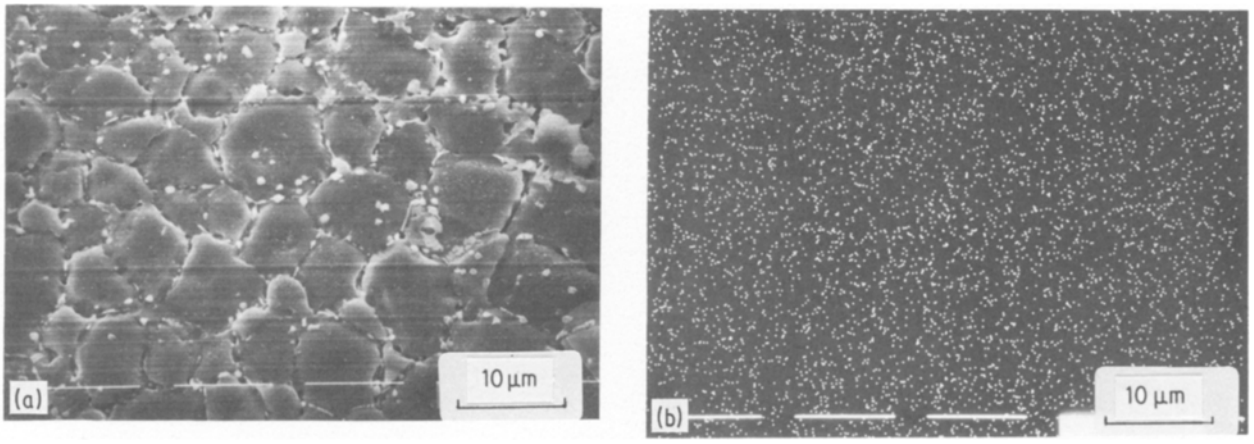

Figure 2 (a) Microstructure and (b) Cr$K\alpha$ X-ray image for hot-pressed 3 mol % Cr_2O_3-doped YSZ.

was observed only in the regions of log [p_{O_2}(Pa)] around zero. In p_{O_2} of both very low and very high values, potential differences did not exhibit such a non-ohmic behaviour and conductivity data could be obtained in those regions from the plot of potential difference against current.

3.2. Variation of conductivity with p_{O_2}

Electrical conductivity dependence on p_{O_2} was examined for 8 mol % Y_2O_3-stabilized ZrO_2 containing 0 to 3 mol % Cr_2O_3. The conductivity results plotted against p_{O_2} are shown in Fig. 4. The conductivities with p_{O_2} seem to be almost constant. Although they showed some fluctuations they did not show a significant and systematic slope compared to the slope of 3/16 which was relevant to the conductivity of Cr_2O_3. Therefore these fluctuations are considered to be due to experimental errors caused mainly by polarization. Thus the conductivity of Cr_2O_3-doped YSZ seems to be almost ionic in the p_{O_2} range studied.

Arrhenius plots of the conductivity in air are shown in Fig. 5. It shows a slight decrease in the conductivity of YSZ on Cr_2O_3 addition. This conductivity decrease may be attributed to the microstructural change on Cr_2O_3 addition. The particles of Cr_2O_3 precipitated on the grain boundaries in these specimens, as seen in Fig. 2. The existence of a secondary phase on the grain boundary generally hinders the ionic conductivity of electrolytes. The Cr_2O_3 precipitated on the grain boundary might have hindered the ionic conduction at the grain boundaries. Since Cr_2O_3 is not an ionic conductor, vacancy trapping or polarization might occur at the grain boundaries. Hence the grain boundary resistivity has been increased with Cr_2O_3 addition.

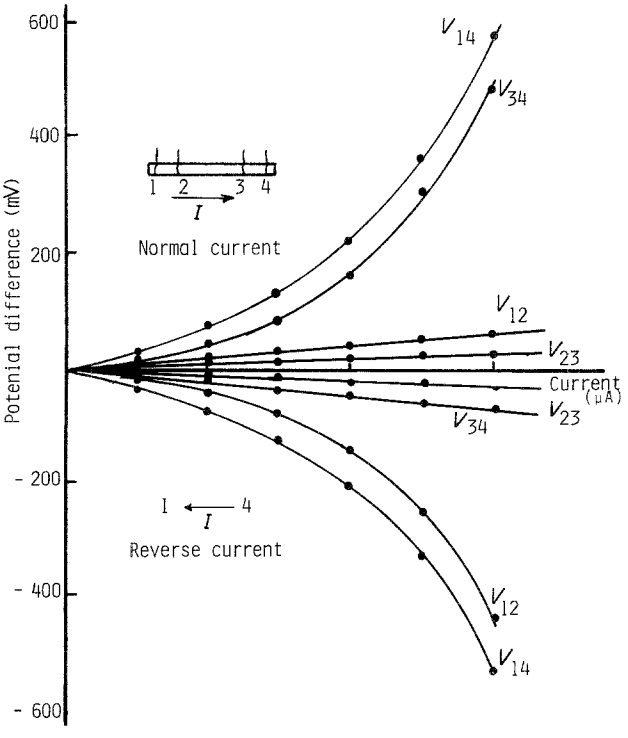

Figure 3 Potential differences between each pair of probes of the sample at 1100° C (1 mol % Cr_2O_3 doped YSZ, in CO_2), indicating cathode polarization in this atmosphere.

Furthermore, Fig. 5 shows that the activation energy for conductivity decreased with Cr_2O_3 addition. Activation energies for conductivities were found to be 0.96, 0.93 and 0.90 eV for 0, 1 and 3 mol % Cr_2O_3 added to YSZ, respectively.

3.3. Variation of conductivity with composition

The conductivities of 1 mol % Cr_2O_3-doped YSZ containing various Y_2O_3 contents were measured at various temperatures. Fig. 6 shows isothermal conductivities plotted against Y_2O_3 contents and Fig. 7 shows Arrhenius plots of these conductivities. They show that the conductivity increases with Y_2O_3 to a maximum conductivity at about 8 mol % Y_2O_3 content and then it decreases with further increasing Y_2O_3 content due to vacancy clustering. Even for pure YSZ a maximum conductivity has been reported in previous studies [4] at compositions of about 8 to 9 mol % Y_2O_3. Thus the variation of the ionic conductivity behaviour of Cr_2O_3-doped YSZ with Y_2O_3 content was similar to that of pure YSZ. The activation energies for conductivity also increased with increasing Y_2O_3 content. The activation energies for 1 mol % Cr_2O_3 added to YSZ were found to be 0.86, 0.93, 1.07, 1.09 and 1.23 eV for 5, 8, 12, 15 and 17 mol % Y_2O_3 compositions, respectively.

The oxygen vacancy concentrations of these specimens were proportional to the stabilizer (Y_2O_3) content in the solid solution. Therefore ionic conduction increases with Y_2O_3 content at the start. But when the vacancy concentration becomes higher vacancies tend to cluster or become ordered. Because of this the conductivity decreased when the stabilizer content

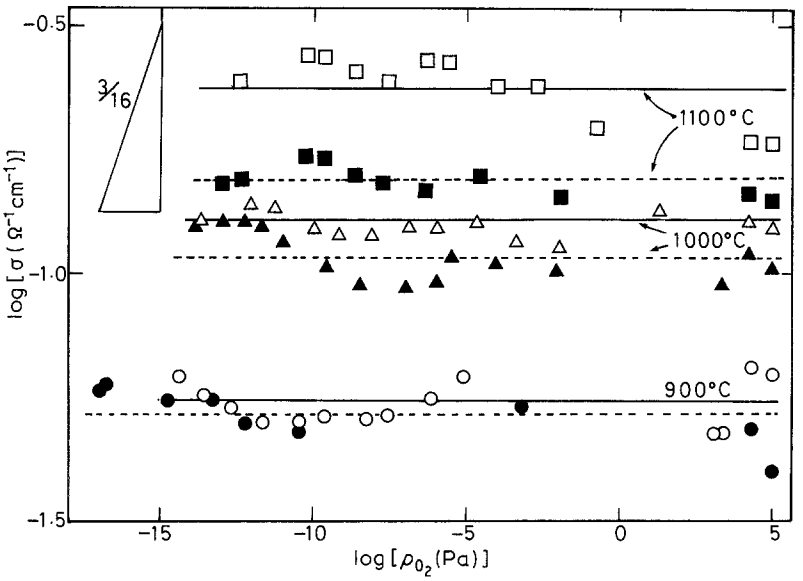

Figure 4 Conductivity dependency on p_{O_2}. Open symbols and solid lines for 1 mol % Cr_2O_3; filled symbols and broken lines for 3 mol % Cr_2O_3 doped YSZ.

increased beyond the maximum amount required to stabilize the cubic phase. Thus in the present study for Cr_2O_3-doped YSZ also the conductivity decreased with an increase of activation energy due to clustering and/or ordering of vacancies when the Y_2O_3 content exceeded 8 mol %.

3.4. Complex impedance

Complex impedance was measured for 3 mol % Cr_2O_3 added to an 8 mol % Y_2O_3-stabilized ZrO_2 sample at the temperatures 224, 280 and 310° C. Impedence plots are shown in Fig. 8. In this case, however, the use of platinum paste did not give a porous electrode surface, so a high resistance was created at the electrode. Thus the results did not distinguish the bulk and grain-boundary resistivities, which was considered to be an effect of the non-porous electrode. However, the first arcs drawn on the d.c. conductivity data agree approximately with these impedance results.

3.5. Defect structure and electrical conductivity

Electrical conductivity in solid electrolytes is primarily determined by the presence of lattice defects [12, 13] whose concentration and mobility are important parameters. Therefore a knowledge of various types of defect such as ionic and electronic is essential to explain the conductivity behaviour.

3.5.1. Stabilized ZrO_2

When Y_2O_3 is added to ZrO_2, Y^{3+} ions substitute to the lattice sites of Zr^{4+} creating oxygen vacancies. The reaction can be written as

$$Y_2O_3 \xrightarrow{ZrO_2} 2Y'_{Zr} + V_O^{\cdot\cdot} + 3O_o \qquad (1)$$

In the intermediate p_{O_2} range, the vacancy concentration is determined by the impurity (Y_2O_3) content and it is much larger than that of the other defects. Therefore the conduction through oxygen

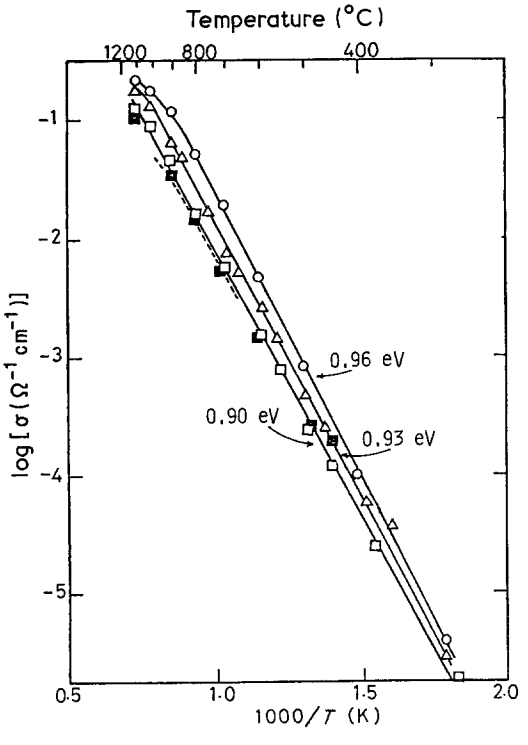

Figure 5 Conductivity of Cr_2O_3-doped YSZ with reciprocal temperature. D.c. values: (○) 0%, (△) 1%, (□) 3% Cr_2O_3; a.c. values (■) 3% Cr_2O_3; (– – –) data from Browall and Doremus [8] for 2% Cr_2O_3.

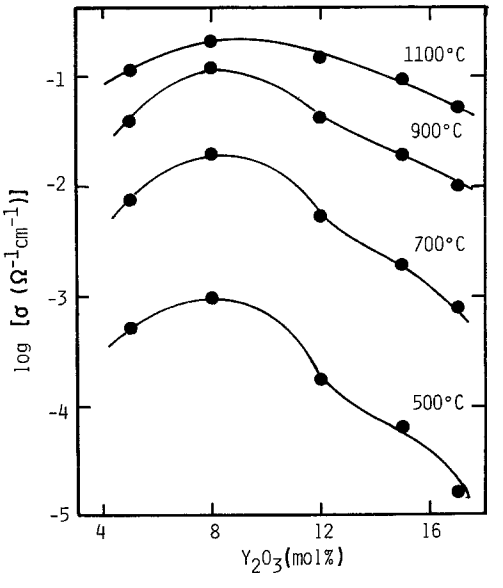

Figure 6 Variation of isothermal conductivity of 1 mol % Cr_2O_3-doped YSZ with Y_2O_3 content.

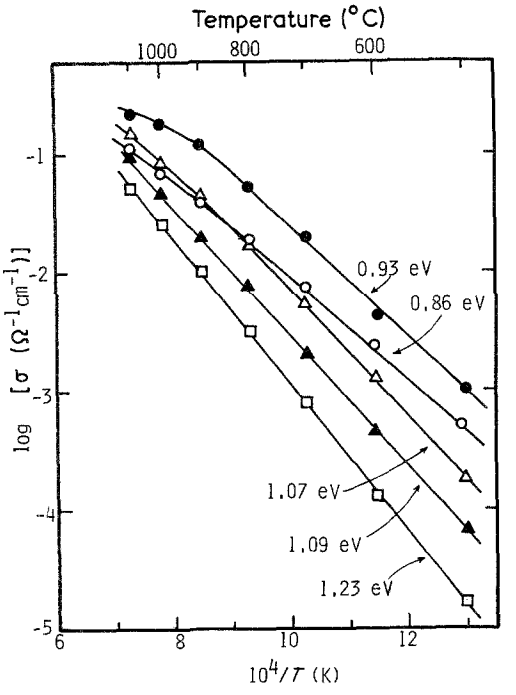

Figure 7 Variation of conductivity of 1 mol % Cr_2O_3-doped ZrO_2 stabilized with various Y_2O_3 contents with reciprocal temperature. Content of Y_2O_3: (○) 5%, (●) 8%, (△) 12%, (▲) 15%, (□) 17%.

ions is usually independent of p_{O_2}. However the ZrO_2 becomes oxygen-deficient depending on the p_{O_2} and temperature as follows [15]:

$$O_o = \tfrac{1}{2}O_2 + V_o^{\cdot\cdot} + 2e' \quad (2)$$

The equilibrium constant K_1 for this reaction is given by

$$K_1 = [V_o^{\cdot\cdot}][e']^2 p_{O_2}^{1/2}$$

But $[V_o^{\cdot\cdot}] = \tfrac{1}{2}[Y'_{Zr}]$ is almost constant according to Equation 1, and therefore

$$[e'] = K'_1 p_{O_2}^{-1/4} \quad (3)$$

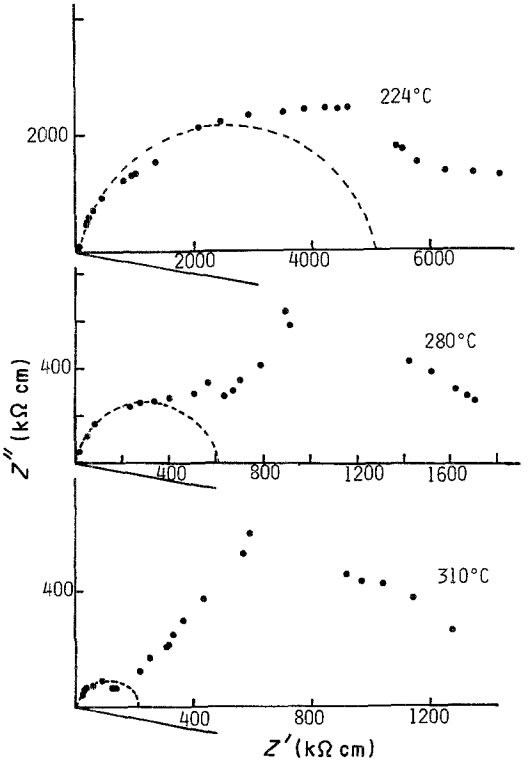

Figure 8 Complex impedence plot for 3 mol % Cr_2O_3-doped YSZ.

Thus at high temperature and low p_{O_2}, n-type conductivity proportional to $p_{O_2}^{-1/4}$ is added to ionic conductivity.

Similarly in very high p_{O_2}, excess oxygen may enter in the place of $V_o^{\cdot\cdot}$ creating $h^{\cdot}$ through the reaction

$$\tfrac{1}{2}O_2 + V_o^{\cdot\cdot} = O_o + 2h^{\cdot} \quad (4)$$

The equilibrium constant K_2 for this reaction is given by

$$K_2 = \frac{[h^{\cdot}]^2}{[V_o^{\cdot\cdot}]p_{O_2}^{1/2}}$$

As $[V_o^{\cdot\cdot}] = [Y'_{Zr}]$ = constant,

$$[h^{\cdot}] = K'_2 p_{O_2}^{1/4} \quad (5)$$

Thus at very high p_{O_2}, it is possible that conductivity occurs through electron holes $[h^{\cdot}]$ and this conductivity will be proportional to $p_{O_2}^{1/4}$. However, these electronic conductivities do not appear in ordinary atmospheres in Y_2O_3-stabilized ZrO_2; they then have almost constant electrical conductivity and it is dominated by the oxygen ion vacancies over a wide range of p_{O_2}.

3.5.2. Cr_2O_3

Pure Cr_2O_3 has p-type conductivity [16] caused by excess oxygen through the reaction

$$\tfrac{3}{2}O_2 = 3O_o + 2V'''_{Cr} + 6h^{\cdot} \quad (6)$$

The equilibrium constant K_3 for this reaction is given by

$$K_3 = \frac{[V'''_{Cr}]^2[h^{\cdot}]^6}{p_{O_2}^{3/2}}$$

and, since $3[V'''_{Cr}] = [h^{\cdot}]$,

$$[h^{\cdot}] = K'_3 p_{O_2}^{3/16} \quad (7)$$

Thus the electrical conductivity of pure Cr_2O_3 is p-type and proportional to $p_{O_2}^{3/16}$.

3.5.3. Cr_2O_3-doped YSZ

When Cr_2O_3 is added to YSZ, Cr^{3+} ions can enter the structure of $Zr_{1-x}Y_xO_{2-x/2}$, either by substitution for cations in the cation sublattice or by taking interstitial positions. In the case of substitution, it forms oxygen vacancies as follows:

$$Cr_2O_3 = 2Cr'_{Zr} + V_o^{\cdot\cdot} + 3O_o \quad (8)$$

and in the case of interstitial solution

$$Cr_2O_3 + 3V_o^{\cdot\cdot} = 2Cr_i^{\cdot\cdot\cdot} + 3O_o \quad (9)$$

In a previous study [12] a solubility of 0.7 mol % Cr_2O_3 in 8 mol % Y_2O_3-stabilized ZrO_2 was observed. Further, the lattice parameter of YSZ decreased with Cr_2O_3 addition. For an interstitial solution, the decrease of lattice parameters cannot be considered. If a substitutional solution was considered, the lattice parameter decrease was in agreement with Vegard's law as a result of the smaller cation (Cr^{3+}, 0.062 nm) substituting for a larger cation (Zr^{4+}, 0.079 nm). Thus it is assumed that Cr_2O_3 dissolved substitutionally according to the Reaction 8. The Cr^{3+} ions dissolved in ZrO_2 solid solution may cause a small electronic

conductivity as a result of its affinity to change the valence state as a transition-metal ion. Thus two possible defect reactions which cause electronic conductivity can be described as follows:

(a) In the high p_{O_2} region

$$Cr'_{Zr} + V_o^{\cdot\cdot} + \tfrac{1}{2}O_2 = O_o + Cr_{Zr} + h^{\cdot} \quad (10)$$

where the equilibrium constant is

$$K_4 = \frac{[Cr_{Zr}][h^{\cdot}]}{[Cr'_{Zr}][V_o^{\cdot\cdot}]p_{O_2}^{1/2}}$$

Since $[Cr_{Zr}] = [h^{\cdot}]$ and $[V_o^{\cdot\cdot}] =$ constant,

$$[h^{\cdot}] = K'_4[Cr'_{Zr}]p_{O_2}^{1/4} \quad (11)$$

(b) In the low p_{O_2} region

$$Cr'_{Zr} + O_o = \tfrac{1}{2}O_2 + V_o^{\cdot\cdot} + Cr''_{Zr} + e' \quad (12)$$

where the equilibrium constant is

$$K_5 = \frac{[V_o^{\cdot\cdot}][Cr''_{Zr}][e']p_{O_2}^{1/2}}{[Cr'_{Zr}]}$$

Since $[Cr''_{Zr}] = [e']$ and $[V_o^{\cdot\cdot}] =$ constant

$$[e'] = K'_5[Cr'_{Zr}]p_{O_2}^{-1/4} \quad (13)$$

Thus the possible electronic conductivities depend on the dissolved Cr_2O_3 content. But the Cr_2O_3 solubility is very small and therefore the electronic conductivity also should be very small compared to the high ionic conductivity caused by high V_o concentration. However, Cr_2O_3 addition might alter the conductivity of YSZ by narrowing the range of ionic conductivity as shown schematically in Fig. 9. Since the results of the present study remained almost constant, the present study has been carried out in this narrow ionic conduction region.

However, this conductivity will also be determined by the microstructure. If the added Cr_2O_3 content was so high that Cr_2O_3 particles could be interconnected, then there would be additional electronic conductivity through the Cr_2O_3 secondary phase.

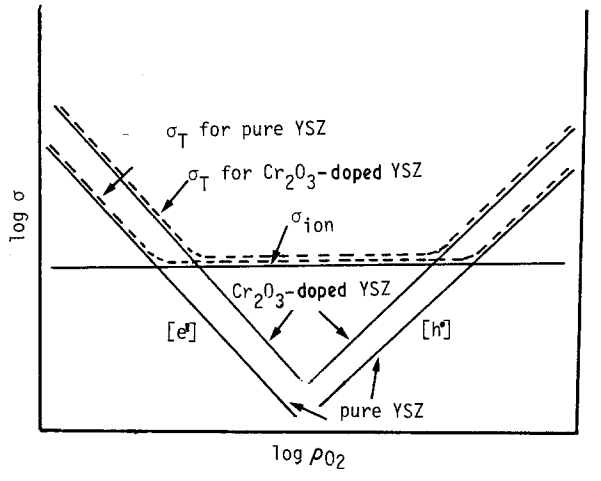

Figure 9 Schematic representation of the conductivity behaviour of Cr_2O_3-doped YSZ compared with pure YSZ.

References

1. K. KIUKKOLA and C. WAGNER, *J. Electrochem. Soc.* **104** (1957) 379.
2. W. D. KINGERY, J. PAPPIS, M. E. DOTY and D. C. HILL, *J. Amer. Ceram. Soc.* **42** (1959) 393.
3. J. M. DIXON, L. D. LAGRANGE, U. MERTEN, C. F. MILLER and J. T. PORTER, *J. Electrochem. Soc.* **110** (1963) 276.
4. D. W. STRICKLER and W. G. CARLSON, *J. Amer. Ceram. Soc.* **47** (1964) 122.
5. E. C. SUBBARAO, in "Advances in Ceramics 3", edited by A. H. Heuer and L. W. Hobbs (American Ceramic Society, Columbus, Ohio, 1981) p. 1.
6. R. V. WILHELM Jr and D. S. HOWARTH, *Ceram. Bull.* **58** (1979) 228.
7. M. HARTMONOVA, L. MACHOVIC, A. KOLLER, F. HANIC and B. MISANKI, *Solid State Ionics* **14** (1984) 93.
8. K. W. BROWALL and R. H. DOREMUS, *J. Amer. Ceram. Soc.* **60** (1977) 262.
9. A. M. ANTHONY, in "Advances in Ceramics 3", edited by A. H. Heuer and L. W. Hobbs (American Ceramic Society, Columbus, Ohio, 1981) p. 437.
10. YU. KARAVAEV, A. M. NEUIMIN, S. F. PAL'GUEV and Z. N. LAKEEVA, *Trans. Inst. Elektrokhim Ural. Nauk. SSSR* No. 23 (1976) 109.
11. M. JAYARATNA, M. YOSHIMURA and S. SŌMIYA, *J. Amer. Ceram. Soc.* **67** (1984) C-240.
12. *Idem, J. Mater. Sci.* **21** (1986) 591.
13. R. N. BLUMANTHAL and M. A. SEITZ, in "Electrical Conductivity of Ceramics and Glass", Part A, edited by N. M. Tallan (Dekker, New York, 1974) p. 35.
14. O. KUBASCHEWSKI, E. L. EVANS and C. B. ALCOCK, "Metallurgical Thermochemistry" (Pergamon, Oxford, 1967) p. 421.
15. E. C. SUBBARAO and H. S. MAITI, *Solid State Ionics* **11** (1984) 317.
16. J. A. CRAWFORD and R. W. VEST, *J. Appl. Phys.* **35** (1964) 2413.

Received 7 July
and accepted 9 September 1986